# Identification of Key Areas for Ecological Conservation and Restoration based on Multi-source Data and Remote Sensing Time Series Analysis

Yuanpeng Chen[1] Xu Zhou*[1] Yan Zhou[1] Chengpeng Zhang[1] Yantao Liu[2] Xiangyan Su[1]
*(1. Land Consolidation and Rehabilitation Center, Ministry of Natural Resource, Beijing 100035 China; 2. Geography and Ocean Science, Nanjing University, School of Nanjing, 210023 China)*

**Keywords:** ecological conservation and restoration, identification of key areas, multi-source data, remote sensing, time series analysis

**Abstract**

Ecological conservation and restoration of national land space is an important aspect for implementing the national ecological civilization strategy, and an important measure for establishing the national ecological security pattern and coordinating the systematic management of mountains, water, forests, fields, lakes, grass and sand. The identification of key areas for ecological conservation and restoration is a precondition to spatially and temporally laying out ecological conservation and restoration planning, which is crucial for the ecological conservation and restoration of national land space. Therefore, this paper considers Henan Province as the study area and carries the research and practice of identifying key areas for ecological conservation and restoration by integrating multi-source data and remote sensing time series analysis. Firstly, based on the Google Earth Engine (GEE) cloud platform and MOD13A1 data, the Mann-Kendall method is used to analyze the trend of time series NDVI in the study area from 2011 to 2020. Secondly, based on multi-source data such as meteorological, soil, topographic, net primary production (NPP), etc., an ecosystem health analysis and assessment based on ecosystem service trade-off and synergy is used to select ecological source. Finally, based on the results of time series NDVI analysis and ecological source selection, fusion analysis is used to identify key areas for ecological conservation and restoration. The results show that this proposed research framework not only considers the "static" ecosystem services and ecosystem health attributes, but also measures the "dynamic" ecosystem change trends. It can effectively identify key areas for ecological conservation and restoration in national space. The results of the study can provide technical support for the background survey, problem identification, planning and engineering layout of ecological conservation and restoration in the national land space.

## 1. Instructions

The ecological protection and restoration of national lands refers to integrated protection and restoration activities of mountains, rivers, forests, fields, lakes, grasslands and deserts in a coordinated and scientific manner in ecological, agricultural and urban spaces where ecological functions are degraded, ecosystems are damaged, spatial patterns are imbalanced, and natural resources are irrationally exploited and utilized following the laws and internal mechanisms of ecosystem succession (Fu Bojie, 2021; Cao Yu et al, 2019; Fang Ying et al, 2020). It is an important lever for the construction of the national ecological civilization, as well as an important measure for building a national ecological security program and coordinating the systematic governance of mountains, rivers, forests, fields, lakes, grasslands, and deserts (Bai Zhongke et al, 2019). As an effective program to enhance the structural and functional integrity of ecosystems, the ecological protection and restoration of national lands has been elevated to a national strategic project (Li Hongju et al, 2019).

The identification of key areas for ecological protection and restoration is of vital importance. It is the foundation for a series of work, including the compilation of protection and restoration plans, the planning and spatiotemporal layout of protection and restoration projects, and the selection of ecological protection and restoration measures (Huang Liping et al, 2023).

Currently, the identification of critical zones for national lands protection and restoration mainly relies on the ecological security pattern constructed by the least cumulative resistance model (Wu Jiansheng et al, 2018; Zhang Meili et al, 2021; Wen Xuejing et al, 2021) or the circuit theory (Cao Xiufeng et al, 2022; Yan Yuyu et al, 2022). The framework model of identifying ecological sources, constructing resistance surfaces, and extracting ecological corridors has become the basic paradigm for the construction of the ecological security programs (Peng Jian et al, 2018), which primarily extracts ecological sources (Peng J et al, 2018). Ecological sources are the starting point for the outward dispersal of species or ecological flows that facilitate ecological processes, maintain system integrity, provide high quality ecosystem services, and serve as key areas for ensuring regional ecological security (Wu Maoquan et al, 2019). Methods for identifying ecological sources can be categorized into direct (Xu W et al, 2021) and comprehensive evaluation methods (Su Chong et al, 2019). Currently, the most commonly used method identifies ecological sources based on multi-indicator ecosystem services and by considering human factors. However, while current protection and restoration plans fully consider the numerical relationships between variables, they gave insufficient consideration to the ecological relationships between variables and the synergy between different ecosystem services (Li Shuangcheng et al, 2013; Fu Bojie, 2016; Cao Qiwen et al, 2016).

Under the current paradigm of ecological security pattern construction, the identification of key areas for ecological protection and restoration in national lands usually starts from a single time node and extracts ecological corridors and strategic points based on the identification of ecological sources. However, ecosystem time-series changes are not considered (Wang Li et al, 2023). Therefore, this study considers the ecosystem service trade-off and synergy in the ecosystem health (EH) assessment and extracts the ecological sources in a more scientific and reasonable manner. Furthermore, the trend of the long-term vegetation index changes are analyzed and the dynamic and static factors of the ecological security program are integrated to comprehensively and accurately identify the key areas of ecological protection and restoration. This provides technical support for the background survey, problem identification, spatial planning and project layout of ecological protection and restoration in national lands.

## 2. Study area and data sources

### 2.1 Overview of the study area

The study area is an ecological protection and restoration project in Henan Province, located in the northern part of the eastern section of the Qinling Mountains and the western part of Henan Province. The geographic coordinates are 33°38'33'' - 35°4'50''N and 110°21'50'' - 113°36'57''E. The terrain and landforms in this area feature drastic changes. A transitional zone from west to east spans the middle and lower mountains of the Qinling Mountains, loess hills and plateaus, Yiluo intermountain basins, and wetlands in the Yellow River tidal flats. The Level 1 landforms are middle mountain areas such as the Western Xiaoqinling and Funiu Mountains. The average elevation is 1000 - 2000 m, with some peaks exceeding 2000 m above sea level. The Level 2 landforms are the low mountain and hilly areas of Xiaoshan and Songshan in the central area, with an average elevation of 200 - 1000 m. Level 3 landforms are the Yiluo Basin and the Yellow River tidal flats in the northeast, with an average elevation of less than 200 m.

The unique regional climatic and geomorphological features have laid a natural foundation for the development and evolution of five types of terrestrial ecosystems, including forests, wetlands, rivers and lakes, farmland, and towns, as well as the spatial pattern of socio-economic development in the target area.

The study area has a predominantly warm-temperate monsoon climate with four distinct seasons and a mean annual temperature of 14.7°C. January is the coldest month with a mean monthly temperature of 0.3°C. July is the hottest with a mean monthly temperature of 27.5°C. The average annual precipitation is 606.9 mm. The precipitation is mainly concentrated in June to September, accounting for 62.4% of the annual precipitation. The average annual evaporation is 1829.10 mm.The geographical location of the study area is shown in Figure 1.

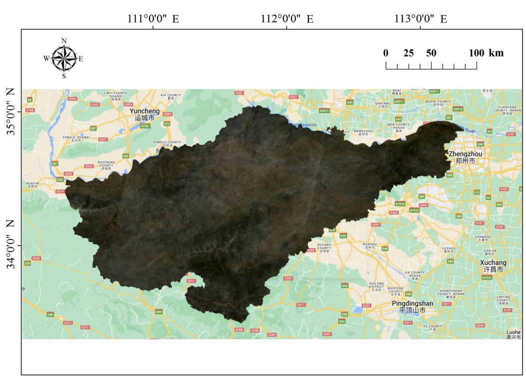


Figure 1. The geographical location of study area

### 2.2 Data source and processing

The data used in this study included meteorological, remote sensing, and land cover data. The meteorological data were obtained from the annual spatial interpolation dataset of meteorological elements in China from the Resource and Environment Science and Data Center of the Chinese Academy of Sciences. The data includes temperature, precipitation, and evaporation for 2020 with a spatial resolution of 1 km. The soil data were obtained from the 1:1 million soil database from the Resource and Environment Science and Data Center. The topographic data were the ground-based digital elevation model data derived from the geospatial data cloud SRTMDEM, with a spatial resolution of 90 m. The remote sensing data were the time-series (2011-2020) normalized difference vegetation index (NDVI) datasets constructed on the basis of MOD13A1, with a total of 230 views and a spatial resolution of 500 m. The land cover data were the MCD12Q1 land cover, a MODIS data product, of which data from 2010, 2015, and 2020 were selected with a spatial resolution of 500 m. The vegetation net primary productivity (NPP) was derived from the MOD17A3HGF dataset (a MODIS data product) for 2011 - 2020 with a spatial resolution of 500 m. Among them, time-series NDVI, NPP, and land cover type data were obtained, and data was batch-processed and calculated through the Google Earth Engine (GEE) cloud platform.

GEE is currently the most advanced cloud computing platform for geospatial observation data such as satellite images. The GEE cloud database stores nearly 40 years of historical data from the Landsat series satellites and provides individual users with powerful computing power and cloud storage space. It also provides a convenient and fast JavaScript language API interface for data processing, algorithm implementation, and result analysis. This study conducted batch processing of remote sensing, land cover, and NPP data required for the study using the GEE cloud computing platform. This reduced the data preprocessing work, effectively improved work efficiency, and decreased the dependence on local hardware devices during data processing and algorithm implementation.

## 3. Research methodology

The research framework of this paper consisted of three main parts. First, based on the GEE cloud platform and the MOD13A1 data, the Mann-Kendall (MK) method was used to carry out trend analysis of the time-series NDVI in the study area from 2011 to 2020. The time-series analysis results were generated. Second, based on the meteorological, topographic, soil, and NPP data, an EH analysis and assessment based on ecosystem service synergy and trade-off calculations was carried out to select ecological sources. Finally, based on the results of the time-series analysis and the selection of ecological sources, overlay analysis was used to identify key areas for ecological protection and restoration. The specific technical roadmap is shown in Figure 2.

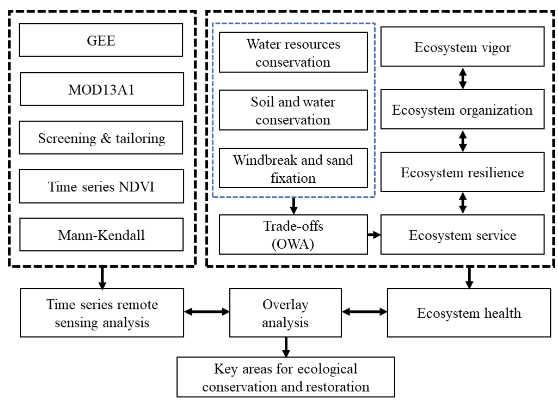



https://doi.org/10.5194/isprs-archives-XLVIII-1-2024-97-2024 | © Author(s) 2024. CC BY 4.0 License.

Figure 2. Workflow of this study

### 3.1 Mann-Kendall trend analysis

The Theil-Sen Median (TSM) trend analysis and the MK non-parametric test method are commonly used to analyze the spatial evolution characteristics of NDVI. In this paper, TSM trend analysis was used in conjunction with the MK test to determine the significance of the TSM trend. Compared with the univariate linear regression trend analysis method, it can avoid the impact of time-series data distribution and missing data on the analysis results, while also reducing the impact of outliers on the results. TSM is calculated as:

$$\beta = Median\left(\frac{NDVI_j - NDVI_i}{j-i}\right),\ 1<i<j<n \quad (1)$$

where $i$, $j$ = time-series number
$NDVI_i$ , $NDVI_i$ = $NDVI$ values for time-series $i$ and $j$
$Median$ = the multi-year NDVI median, $n$ is the time-series length
MK = a nonparametric statistical test used to determine the significance of a trend. The equation is

$$Zc = \begin{cases} \frac{\tau-1}{\sqrt{Var(\tau)}} & (\tau>0) \\ 0 & (\tau>0) \\ \frac{\tau+1}{\sqrt{Var(\tau)}} & (\tau<0) \end{cases} \quad (2)$$

$$\tau = \sum_{i=1}^{n-1}\sum_{j=i+1}^{n} \operatorname{sign}\left(NDVI_j - NDVI_i\right) \quad (3)$$

where $i$, $j$ = the time-series number
$NDVI_i$ , $NDVI_i$ = NDVI values for time-series $i$ and $j$
$n$ = the time-series length

In this paper, we used a significance level of $\alpha$ = 0.05, which corresponded to $u_{1-\alpha/2}$ of 1.96 (Yuan Liuhua et al, 2013).

### 3.2 Ecological source identification based on ecosystem health

This paper performed an EH assessment and identified ecological sources based on ecosystem service trade-offs and synergies.

**3.2.1 Ecosystem health assessment system**: Ecological sources are habitat patches that play a decisive role in regional ecological processes and functions. They provide essential services and are important for the health and safety of regional ecosystems. EH assessments are the basis of ecological source identification. This paper constructed an evaluation framework system from four dimensions: ecosystem vigor (V), ecosystem organization (O), ecosystem resilience (R), and ecosystem service (ES). The equations are

$$EH = \sqrt{PH\ ES} \quad (4)$$

$$PH = \sqrt[3]{OVR} \quad (5)$$

where $PH$ = the ecosystem physical health
$ES$ = the ecosystem service
$V$ = the ecosystem vigor
$O$ = the ecosystem organization
$R$ = the ecosystem resilience

The calculation results of $ES$, $V$, $O$, and $R$ were all normalized.

$V$ was characterized by NPP as it is a good indicator of the efficiency of plants in fixing and converting photosynthetic products and can characterize the material and energy available for human use.

$O$ represents the stability of the regional ecosystem structure, which mainly includes the landscape heterogeneity and connectivity. Additionally, the landscape pattern indices including Area Weighted Mean Patch Fractal Dimension (*AWMPFD*), Shannon Diversity Index (*SHDI*), Contagion Index (*CONT*), and Landscape Fragmentation Index (*FN*) were selected to characterize $O$. The equation is as follows

$$O = 0.3SHDI + 0.2AWMPFD + 0.25FN + 0.25CONT \quad (6)$$

In Equation (6), the landscape pattern indices were calculated using the Fragstats software.

$R$ represents the capability of an ecosystem to maintain its own structural stability in the face of anthropogenic perturbations. It reflects the capability of a region to resist and adapt to external disturbances in ecosystem processes. Thus, it includes two aspects, namely, resistance and resilience (Xie X et al, 2021), which were assigned the values of 0.6 and 0.4, respectively (Li C et al, 2023). To reflect the resilience of different ecosystems of the same land cover type, the correction was made by using NDVI. The equation is

$$R_i = \frac{NDVI_m}{NDVI_{meanj}} \times 0.4Resil_j \times 0.6Resis_j \quad (7)$$

where $R_i$ = the total elasticity coefficient of the $i^{th}$ pixel
$NDVIm$ = the $NDVI$ value of the $m^{th}$ pixel
$NDVImeanj$ = the mean NDVI value of the $j^{th}$ land cover type

$Resilj$ and $Resisj$ are the resilience and resistance coefficients of the $j^{th}$ land cover type, shown in Table 1.

| Land use type | Farmland | Forest | Grassland | Water | Built-up land | Other |
|---|---|---|---|---|---|---|
| Resilience coefficient | 0.4 | 0.9 | 0.7 | 0.8 | 0.2 | 0.1 |
| Resistance coefficient | 0.6 | 1 | 0.6 | 0.8 | 0.3 | 0.2 |

Table 1. Ecological resilience coefficient of land use types

$ES$ represents ecosystem service, which is the bridge between natural and socioeconomic systems (Fu B, 2020). It reflects the coupled relationship between humans and nature and is an important component of EH. In view of the natural and ecological conditions of the study area, this paper selected three types of ecosystem services, namely water resources conservation, soil and water conservation, and windbreak and sand fixation, as the key ecosystem service functions of the area for quantitative assessment. These were calculated using the quantitative indicator evaluation method with NPP. The equation is

$$WR = NPP_{mean} F_{sic} F_{pre} \left(1 - F_{slo}\right) \quad (8)$$


https://doi.org/10.5194/isprs-archives-XLVIII-1-2024-97-2024  

where $WR$ = the ecosystem water conservation service capability index
$NPP_{mean}$ = the average NPP of vegetation
$F_{sic}$ = the soil percolation factor
$F_{pre}$ = the average precipitation factor
$F_{slo}$ = the slope factor

$$S_{pro} = NPP_{mean}\left(1-K\right)\left(1-F_{slo}\right) \tag{9}$$

where $S_{pro}$ = the ecosystem soil and water conservation service capability index
$NPP_{mean}$ = the average NPP
$F_{slo}$ = the slope factor
$K$ = the soil erodibility factor.

$$\begin{gathered} S_{ws} = NPP_{mean} K F_q D \\ F_q = \frac{1}{100}\sum_{i=1}^{12} u^3\left(\frac{ETP_i - P_i}{ETP_i}\right) d \\ ETP_i = 0.19\times\left(20+T_i\right)^2\left(1-r_i\right) \\ D = 1/cos\left(\theta\right) \end{gathered} \tag{10}$$

where $S_{ws}$ = the ecosystem windbreak and sand fixation service capability index
$F_q$ = the average climatic erosivity
$u$ = the monthly average wind speed at a height of 2 m
$ETP_i$ = the monthly potential evaporation
$P_i$ = the monthly precipitation
$d$ = the number of days in the month
$T_i$ = the average monthly temperature
$r_i$ = the monthly average relative humidity given in %
D = the surface roughness factor
$\theta$ = the slope given in *rad*

**3.2.2 Ecosystem service trade-offs and synergies**: In the context of ecosystem services, the selection of ecological sources must take full account of ecosystem trade-offs and synergies. The ordered weighted average model (OWA) has been effectively used to quantify the trade-offs and synergies between ecosystem services. Therefore, OWA can quantify the supply of ecosystem services in different scenarios, reflecting the trade-offs and synergies between different ecosystem services. The equation is as follows.

$$\begin{gathered} OWA\left(a_{xj}\right) = \sum_{x}^{N} \omega_x S_{xj} \\ \left(\omega_x \in \left[0,1\right] \text{ 且 } \sum_{x}^{N} \omega_x = 1,\ j = 1,2,\cdots,N\right) \end{gathered} \tag{11}$$

In addition, two parameters of risk and trade-off were used as constraints and optimization conditions for OWA. The equation is

$$risk = \left(M-1\right)^{-1}\sum_{x}^{M}\left(M-x\right)\omega_x \quad \left(0 \le risk \le 1\right) \tag{12}$$

$$\max\ trade-off = 1-\sqrt{\frac{M\sum_{x}^{M}\left(\omega_x - \frac{1}{M}\right)^2}{M-1}}, \quad \left(0 \le tradeoff \le 1\right) \tag{13}$$

$$\sum_{x}^{M}\omega_x = 1 \ \left(\omega_x \in \left[0-1\right]\right) \tag{14}$$

where $a_{xj}$ = the attribute value of the $j^{th}$ pixel in the $x^{th}$ raster data
$S_{xj}$ = the raster data after reweighing
$\omega_x$ = the weight of $S_{xj}$
$M$ = the volume of ecosystem service raster data involved in the calculation.

By calculating risk and trade-off values, the optimal combination of ecosystem service weight coefficients for different scenarios can be obtained. The maximum trade-off values and the corresponding weights were calculated and a total of 11 scenarios were set.

**3.2.3 Ecological source identification**: To effectively select ecological sources for different scenarios, the areas with the top 60% of EH values were selected as the priority protection areas. Ecological sources in priority protection areas were further screened using the ecosystem protection efficiency equation. The equation is as follows.

$$E_i = \frac{\overline{EH}_{ic}}{\overline{EH}_{is}} \tag{15}$$

where $\overline{EH}_{ic}$ = the average health value of the $i$-class ecosystem in the priority protection area
$\overline{EH}_{is}$ = the average health value of the $i$-class ecosystem in the whole study area

### 3.3 Identification of critical areas for ecological protection and restoration

Based on the downward, stable and slightly upward trends of NDVI in the time-series remote sensing trend analysis, as well as the results of EH assessment and ecological source identification, the overlay analysis was applied to further identify key areas for ecological protection and restoration.

## 4. Results and analysis

### 4.1 Time-series remote sensing trends

The time-series NDVI data of the study area from 2011 to 2020 were obtained from the GEE cloud platform, with a total of 230 scenes. Based on the statistical description, the mean values of the NDVI data of 230 scenes fluctuated within the range of 0.16 to 0.76. Also, the fluctuation cycle conformed to the characteristics of the annual seasonal phase. The standard deviation fluctuated in the range of 0.06 to 0.23, with good stability and data quality. The results of the time-series NDVI data construction were as expected.

Based on the TSM trend analysis combined with the MK nonparametric test, the statistical data and spatial distribution of time-series NDVI trend changes were formed at the significance level of $\alpha$ = 0.05 (Figure 3). First, the slope change range of time-series NDVI within the study area was determined at -0.0017 - 0.0021, with a mean of 0.0003. Among them, 6136 pixels had negative slopes, accounting for 5.33%. This indicated that during the period of 2011 - 2020, the NDVI of a few local areas in the study area showed a downward trend, but the overall NDVI change showed an upward trend. This reflected the stable and improving quality of the ecosystem in the study area to some extent. Second, by overlaying land cover types, the spatial distribution of NDVI trend changes shows that the areas with a downward trend in NDVI from 2011 to 2020 were mainly distributed in concentrated areas of impermeable surfaces and surrounding buffer areas along the Luo and Yi Rivers in the central region, the Yellow River in the northeast, and in the piedmont plain on the north side of the Xiaoqinling Mountains in the northwest. Some scattered distribution was identified in other areas as well. The areas with an upward trend in NDVI were mainly distributed in the central loess hills and eastern intermountain basins. The main types of land cover were arable land, grassland, and a small amount of shrubland. Areas with insignificant NDVI variation trends were mainly distributed in the middle and lower mountainous regions of the Qinling Mountains, including Xiaoshan, Xiong’er, and Funiu mountains. The land cover types were dominated by forests.

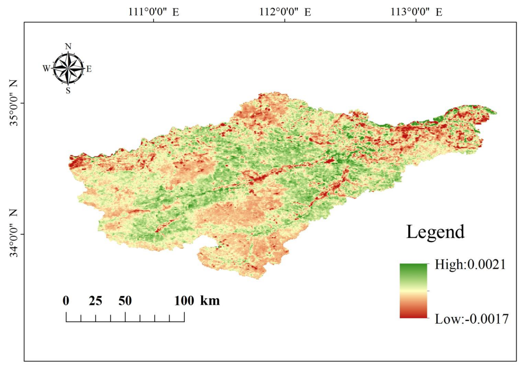


(a) NDVI trend

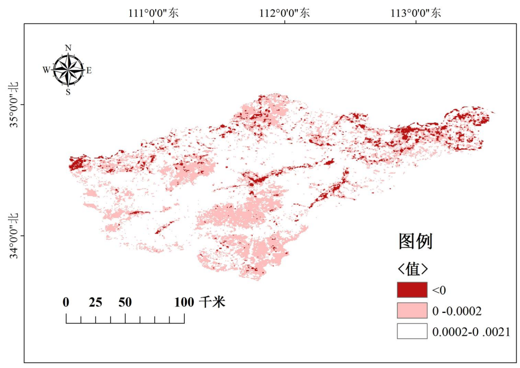


(b) NDVI trend (dominated by the negative trend)

Figure 3. Trend of time-series normalized difference vegetation index (NDVI) data

## 4.2 Results of the ecosystem health assessment

**4.2.1 Ecosystem physical health**: V, O and R were calculated according to Equations (5) to (7). After normalization, further calculations were conducted to obtain the evaluation results and spatial distribution of ecosystem physical health (Figure 4). Figure 6 shows the mean value of the physical health of the ecosystem was 0.592. The high value areas in the study area were mainly distributed in the middle and lower mountainous areas of the Qinling Mountains on the west side, such as the Xiaoqinling, Xiong’er, and Funiu Mountains. The vegetation in the middle and lower mountainous areas generally grew well and the EH level was high. From west to east, the physical health value of the ecosystem gradually decreased. Low value areas were mainly distributed in areas with severe soil erosion, such as the Yiluo intermountain basin and tidal flats along the rivers. In addition, more urbanized areas had lower levels of ecosystem physical health due to greater disturbance from human activities.

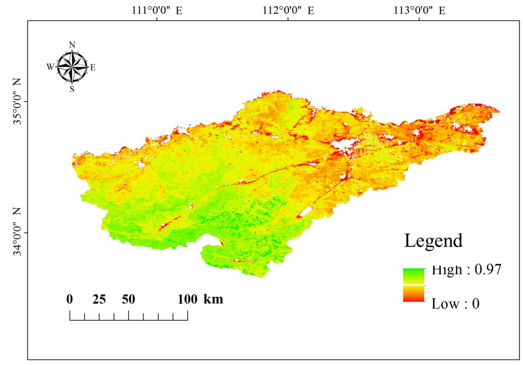


Figure 4. Spatial distribution of ecosystem physical health

**4.2.2 Ecosystem services**: According to the quantitative indicator evaluation algorithms of NPP in Equations (8) to (10) and after normalization, the evaluation results and spatial distribution of ecosystem services were obtained (Figure 5). The existence of spatial heterogeneity among different ecosystem service capacities reflected the trade-offs among service capacities. It also revealed the impact of different ecological processes on the overall ecological security pattern of the study area. As shown in Figure 5, the water conservation service capacity in the study area gradually decreased from southwest to northeast. The areas with stronger water conservation capacity were mainly distributed in the middle and lower mountainous areas. However, not all middle and lower mountainous areas had stronger water conservation service capacity. Stronger areas were mainly concentrated in the region of Funiu, Xiong’er, and Waifang Mountains. Compared with the water conservation capacity, the distribution of soil and water conservation capacity was relatively balanced. The important areas were mainly located in the middle and lower mountains, loess hills and the areas around the Luhun Reservoir. A certain synergy was identified between the windbreak and sand fixation capacity and the water resources conservation capacity. The stronger areas were mainly concentrated in the middle and lower mountainous areas, of which the strongest areas were distributed in the Xiaoqinling, Xiong’er and Funiu Mountains. The second strongest areas were the Xiaoshan, Qingyao, Waifang and Songshan Mountains. In terms of the spatial patterns of single ecosystem services, the areas with stronger ecosystem service capacity within were mainly distributed in areas with higher elevations and stronger vegetation cover, such as the middle and lower mountainous areas and loess hilly areas.

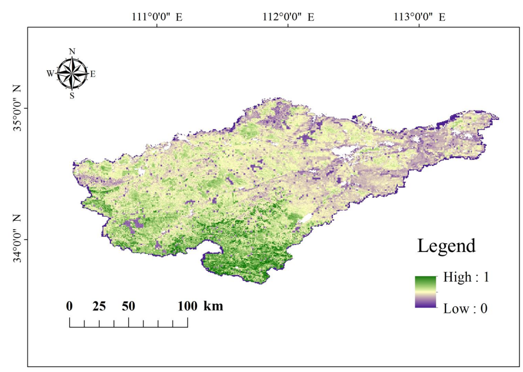


(a) Water resources conservation service capacity

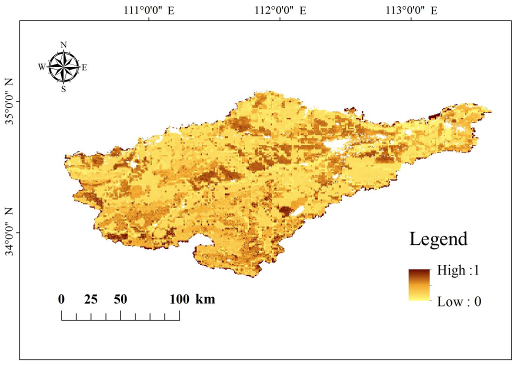


(b) Soil and water conservation service capacity

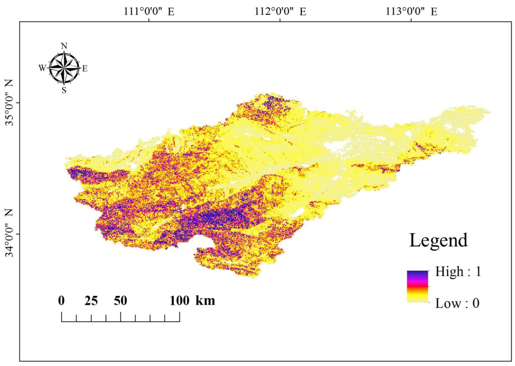


(c) Windbreak and sand fixation service capacity

Figure 5. Spatial distribution of different ecosystem services

**4.2.3 Ecosystem service synergies and trade-offs**: According to the ecosystem service trade-off and synergy algorithms in Equations (11) to (14), a series of scenarios can be generated by changing the decision risk as well as the synergy and trade-off values. Based on the actual work, the risk values were set with 0 as the starting point and 0.1 as the interval. The maximum synergy and trade-off values and their corresponding weight were calculated to obtain a total of 11 scenarios (Table 2).

| Scenario | Risk | Trade-off | $\omega_1$ | $\omega_2$ | $\omega_3$ |
|---|---|---|---|---|---|
| 1 | 0 | 0.423 | 0 | 0 | 1 |
| 2 | 0.1 | 0.584 | 0 | 0.200 | 0.800 |
| 3 | 0.2 | 0.7 | 0.033 | 0.333 | 0.633 |
| 4 | 0.3 | 0.8 | 0.133 | 0.333 | 0.533 |
| 5 | 0.4 | 0.9 | 0.233 | 0.333 | 0.433 |
| 6 | 0.5 | 1 | 0.333 | 0.333 | 0.333 |
| 7 | 0.6 | 0.9 | 0.433 | 0.333 | 0.233 |
| 8 | 0.7 | 0.8 | 0.533 | 0.333 | 0.133 |
| 9 | 0.8 | 0.7 | 0.633 | 0.333 | 0.033 |
| 10 | 0.9 | 0.584 | 0.800 | 0.200 | 0 |
| 11 | 1 | 0.423 | 1 | 0 | 0 |

Table 2. Optimal order weights for different decision risk scenarios and trade-off levels

**4.2.4 Ecosystem health assessment and ecological source identification results**: Based on the calculation results of ecosystem physical health and services, combined with the 11 scenarios of ecosystem service trade-offs and synergies, the health assessments and their spatial distribution characteristics were calculated according to Equation (4)

As shown in Figure 8, the spatial distribution of high and low values of EH showed a consistent trend, but there were some differences in local high and low value areas. This was due to different scenarios and ecosystem service trade-off and synergy levels, resulting in different weights. To an extent, it indicates that simple weighted summation cannot fully reflect the spatial distribution of regional EH. Therefore, the synergy and trade-off effects of ecosystem services had to be incorporated into EH assessments.

Based on the EH assessment results of the 11 scenarios, the priority areas for protection under different scenarios were screened according to the top 60% of the high values. Their conservation efficiency was measured according to Equation (15) (Table 3). As shown in Table 3, Scenario 9 had the highest conservation efficiency of 3.02. Therefore, the top 60% high-value areas in Scenario 9 were selected as the ecological source. The spatial distribution is shown in Figure 6. The ecological source in the study area was about 1386.11 km$^2$, mainly distributed in the Funiu, Xiong'er, and Waifang Mountains in the southwest. A small amount was distributed in the Xiaoqinling area. The land cover types involved were mainly forest and grassland.

| Scenario | 1 | 2 | 3 | 4 | 5 | 6 |
|---|---|---|---|---|---|---|
| $E_i$ | 1.02 | 1.37 | 1.78 | 1.85 | 2.21 | 2.18 |
| Scenario | 7 | 8 | 9 | 10 | 11 | |
| $E_i$ | 2.23 | 2.41 | 3.02 | 2.96 | 1.87 | |

Table 3. Protection efficiency of priority protected areas in different scenarios

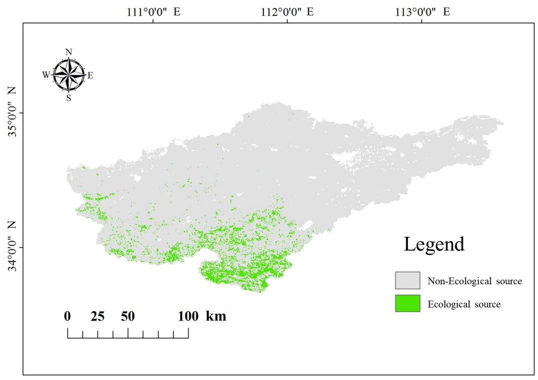


Figure 6. Spatial distribution of ecological sources in study area.

## 4.3 Critical areas for ecological protection and restoration

Based on the results of the time-series remote sensing trend analysis (Figure 3), areas with NDVI in the decreasing trends (slope less than 0) as well as in the stable and slightly increasing trends (slope between 0 and 0.0002) were selected and overlaid with the selected ecological sources (Figure 6).

The areas with stable and slightly increasing NDVI and the ecological sources were combined as the key areas for ecological protection. ① The ecological sources where NDVI remained stable or slightly increased were designated as the first-class ecological protection areas. The reason was that these areas are important for maintaining EH. From the time-series perspective, NDVI can characterize ecosystems that have not shown a significant trend of change in the past 10 years and have been in a critical state. If not designated as a key protection area, there may be further ecosystem degradation or destruction. Therefore, these areas must be a primary ecological protection area to gradually form ecosystem stability and a steady increase in NDVI. ② The ecological sources where NDVI increased were designated as the second-class ecological protection areas, which were also important areas to maintain the health of the ecosystem. As opposed to the primary ecological protection areas, NDVI in secondary protection areas had formed an upward trend in the last 10 years, and the ecosystem had been stabilized. ③ Areas with stable and slightly increasing NDVI that did not overlap with the ecological sources were designated as the tertiary ecological protection areas. Compared with the primary and secondary ecological protection areas, the tertiary ecological protection areas did not include the ecological sources. Their contribution to maintaining the integrity of the ecosystem and providing high quality ecosystem services in the areas was relatively weak. The ecosystems in such areas had not been significantly damaged during the past 10 years. Therefore, protecting these areas to maintain the status quo or gradually transform them into areas with stronger ecosystem stability with a steady increase in NDVI was necessary. ④ Areas with declining NDVI were designated as ecological restoration areas where appropriate restoration measures must be implemented. The identification results of the key areas for ecological protection and restoration and their spatial distributions are shown in Figure 7.

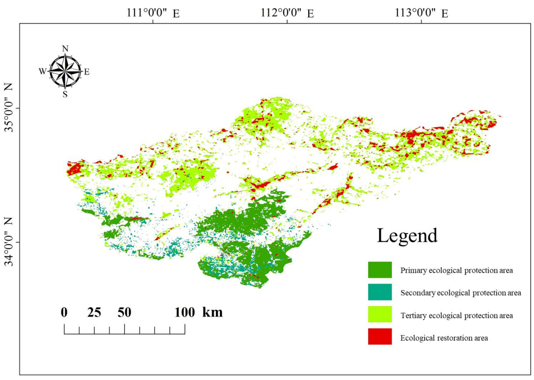


Figure 7. Spatial distribution of ecological protection and restoration key areas identification results.

Figure 10 shows that the first- and second-class ecological protection areas are mainly distributed in the Xiaoqinling, Xiong'er, and Funiu Mountains in the west and southwest. They are mainly characterized by a middle mountain forest ecosystem. These participate in ecosystem services such as biodiversity protection, carbon sequestration, and oxygen release. The third-class ecological protection areas are mainly distributed in the Mangshan and Xiaoshan Mountains. There are also sporadic distributions in the Yiluo Basin and the tidal flats of the Yellow River. These mainly consist of low mountain and hilly forest ecosystems, intermountain basin farmland ecosystems, and river ecosystems. They can provide ecosystem services such as water resources conservation, soil and water conservation, carbon sequestration and oxygen release, mineral resource provision, and agricultural and forestry product provision. The ecological restoration areas are mainly distributed in the concentrated areas of impermeable surfaces and surrounding buffer areas along the Luo River and Yi River in the central areas, the Yellow River in the northeast, and the piedmont plain on the north side of the Xiaoqinling Mountains in the northwest corner. These are mainly urban, agricultural, and river ecosystems in the basin area. They participate in ecosystem services such as agricultural product provision and urban ecological conservation.

## 5. Conclusion

This study effectively identified the key areas for ecological protection and restoration in the study area based on methods such as time-series remote sensing analysis, ecosystem service synergy and trade-off calculation, EH assessment, ecological source identification, and spatial overlay analysis. This not only considered the static ecosystem services and EH attributes within the research area, but also measured the dynamic trend of ecosystem changes. This enables a more comprehensive and accurate identification of key areas for ecological protection and restoration. The research results can provide technical support for the background survey, problem identification, and planning and engineering layout of ecological protection and restoration of national land space.

## References

Bai Zhongke, Zhou Wei, Wang Jinman, et al, 2019: Overall protection, systematic restoration and comprehensive management of land space [J]. *China Land Science*, 33(2): 1-11.

Cao Qiwen, Wei Xiaomei, Wu Jiansheng, 2016: A review on the tradeoffs and synergies among ecosystem services [J]. *Chinese Journal of Ecology*, 35(11): 3102-3111.

Cao Xiufeng, Liu Zhaoshun, Li Shujie, et al, 2022: Identification of key areas of ecological protection and restoration based on the pattern of ecological security: a case of Songyuan City, Jilin province [J]. *China Environmental Science*, 42(6): 2779-2787.

Cao Yu, Wang Jiayi, Li Guoyu, 2019: Ecological restoration for territorial space: basic concepts and foundations [J]. *China Land Science*, 33(7): 1-10.

Fang Ying, Wang Jing, Huang Longyang, et al, 2020: Determining and identifying key areas of ecosystem preservation and restoration for territorial spatial planning based on ecological security patterns: a case study of Yantai City [J]. *Journal of Natural Resources*, 35(1): 190-203.

FU B, 2020: Promoting geography for sustainability [J]. *Geography and Sustainability*, 1(1): 1-7.Fu Bojie, 2021: Several key points in territorial ecological restoration. *Bulletin of Chinese Academy of Sciences*, 36(1): 64-69.

Fu Bojie, Yu Dandan, 2016: Trade-off analyses and synthetic integrated method of multiple ecosystem services [J]. *Resources Science*, 38(1): 1-9.

Fu Fengjie, Liu Zhenhuan, Liu Hai, 2021: Identifying key areas of ecosystem restoration for territorial space based on ecological security pattern: a case study in Hezhou City [J]. *Acta Ecologica Sinica*, 41(9): 3406-3414.

GORELICK N, HANCHER M, DIXON M, et al, 2017: Google Earth Engine: planetary-scale geospatial analysis for everyone [J]. *Remote Sensing of Environment*, 202: 18-27.

Huang Liping, Xiang Fangfang, Chen Rongqing, 2023: Identification of key areas for ecological protection and restoration of county territorial space based on ecological security pattern: a case study in Yihuang County of Fuzhou City[J]. *Journal of Environmental Engineering Technology*, 13(4): 1334-1344.

LI C, WU Y, GAO B, et al, 2023: Construction of ecological security pattern of national ecological barriers for ecosystem health maintenance [J]. *Ecological Indicators*, 146: 109801.

Li Hongju, Yu Zhenrong, Liang Jun, et al, 2019: Study on the unified standard system of ecological protection and rehabilitation of mountain-river-forest-farmland-lake-grass [J]. *Acta Ecologica Sinica*, 39(23): 8771-8779.

Li Shuangcheng, Zhang Yucai, Liu Jinlong, et al, 2013: The tradeoffs and synergies of ecosystem services: research progress, development trend, and themes of geography [J]. *Geographical Research*, 32(8): 1379-1390.

Peng J, Yang Y, Liu Y, et al, 2018: Linking ecosystem services and circuit theory to identify ecological security patterns [J]. *Science of the Total Environment*, 644: 781-790.

Peng Jian, Li Huilei, Liu Yanxu, et al, 2018: Identification and optimization of ecological security pattern in Xiong'an New Area [J]. *Acta Geographica Sinica*, 73(4): 701-710.

PRASAI R, SCHWERTNER T W, MAINALI K, et al, 2021: Application of Google Earth Engine python API and NAIP imagery for land use and land cover classification: a case study in Florida, USA [J]. *Ecological Informatics*, 66: 101474.

Su Chong, Dong Jianquan, Ma Zhigang, et al, 2019: Identifying priority areas for ecological protection and restoration of mountainsrivers-forests-farmlands-lakes-grasslands based on ecological security patterns: a case study in Huaying Mountain, Sichuan Province [J]. *Acta Ecologica Sinica*, 39(23): 8948-8956.

Wang Li, Zhao Siyan, Chen Yuanpeng, et al, 2023: Vegetation change and attribution in ecological restoration area of Loess Plateau Based on GEE cloud platform [J]. *Transactions of the Chinese Society for Agricultural Machinery*, 54(3): 210-223.

Wen Xuejing, Zhou Zhi, Zhang Meili, et al, 2021: Identification of key areas of territorial ecological restoration in Taihang Mountains — a case study of Tang County [J]. *Chinese Journal of Eco-Agriculture*, 29(12): 2093-2106.

Wu Jiansheng, Ma Hongkun, Peng Jian, 2018: Improving urban ecological security pattern based on functional nodes-key corridors: a case study of Shenzhen City [J]. *Progress in Geography*, 37(12): 1663-1671.

Wu Maoquan, Hu Mengmeng, Wang Tao, et al, 2019: Recognition of urban ecological source area based on ecological security pattern and multi-scale landscape connectivity [J]. *Acta Ecologica Sinica*, 39(13): 4720-4731.

XIE X, FANG B, XU H, et al, 2021: Study on the coordinated relationship between urban land use efficiency and ecosystem health in China [J]. *Land Use Policy*, 102: 105235.

Yan Yuyu, Sun Yanwei, Liu Min, 2022: Identification and restoration strategy of key areas for territorial space ecological restoration in Shanghai, China based on ecological security pattern [J]. *Chinese Journal of Applied Ecology*, 33(12): 3369-3378.

Yuan Liuhua, Jiang Weiguo, Shen Wenming, et al, 2013: The spatio-temporal variations of vegetation cover in the Yellow River Basin from 2000 to 2010 [J]. *Acta Ecologica Sinica*, 33(24): 7798-7806.

Zhang Meili, Li Zhi, Zhang Yichen, et al, 2021: Identification of key areas of ecological restoration of land and space based on ecological security pattern-taking Fuping Country of Hebei Province as an example [J]. *Research of Soil and Water Conservation*, 28(3): 299-307.